the solvent compositions, where the X-ray scattering measurements were performed with solutions containing 100 mM NH_4Cl.

References

Abrahamson, J. K., Laue, T. M., Miller, D. L., & Johnson, A. E. (1985) *Biochemistry 24*, 692–700.

Antonsson, B., & Leberman, R. (1984) *Eur. J. Biochem. 141*, 483–487.

Antonsson, B., Kalbitzer, H. R., & Wittinghofer, A. (1981) *Hoppe-Seyler's Z. Physiol. Chem. 362*, 735–743.

Arai, K.-I., Kawakita, M., Kaziro, Y., Kondo, T., & Ui, N. (1973) *J. Biochem. (Tokyo) 73*, 1095–1105.

Boutorin, A. S., Clark, B. F. C., Ebel, J. P., Kraus, T. A., Petersen, H. U., Remy, P., & Vassilenko, S. (1981) *J. Mol. Biol. 152*, 593–608.

Dessen, P., Blanquet, S., Zaccai, G., & Jacrot, B. (1978) *J. Mol. Biol. 126*, 293–313.

Dessen, P., Fayat, G., Zaccai, G., & Blanquet, S. (1982) *J. Mol. Biol. 154*, 603–613.

Ehresmann, B., Imbault, P., & Weil, J. H. (1971) *Anal. Biochem. 54*, 454–463.

Guinier, A., & Fournet, G. (1955) *Small Angle Scattering of X-rays*, Wiley, New York.

Holmes, W. M., Hurd, R. E., Reid, B. R., Rimerman, R. A., & Hatfield, G. W. (1975) *Proc. Natl. Acad. Sci. U.S.A. 72*, 1068–1071.

Ibel, K. (1976) *J. Appl. Crystallogr. 9*, 630–643.

Jacrot, B., & Zaccai, G. (1981) *Biopolymers 20*, 2413–2426.

Jones, M. D., Petersen, T. E., Nielsen, K. M., Magnusson, S., Sotterup-Jensen, L., Gausing, K., & Clark, B. F. C. (1980) *Eur. J. Biochem. 108*, 507–526.

Kabsch, W., Gast, W. H., Schulz, G. E., & Leberman, R. (1977) *J. Mol. Biol. 117*, 999–1012.

Leberman, R., Giovanelli, R., & Acosta, Z. (1974) *Nucleic Acids Res. 1*, 1007–1016.

Leberman, R., Wittinghofer, A., & Schulz, G. E. (1976) *J. Mol. Biol. 106*, 951–961.

Leberman, R., Antonsson, B., Giovanelli, R., Guariguata, R., Schumann, R., & Wittinghofer, A. (1980) *Anal. Biochem. 104*, 29–36.

Li, Z. Q., Giegé, R., Jacrot, B., Oberthür, R., Thierry, J.-C., & Zaccai, G. (1983) *Biochemistry 22*, 4380–4388.

Louie, A., & Jurnak, F. (1985) *Biochemistry 24*, 6433–6439.

Louie, A., Ribiero, N. S., Reid, B. R., & Jurnak, F. (1984) *J. Biol. Chem. 259*, 5010–5016.

Österberg, R., Sjöberg, B., Ligaarden, R., & Elias, P. (1981) *Eur. J. Biochem. 117*, 155–159.

Pingoud, A., Urbanke, C., Krauss, G., Peters, F., & Maass, G. (1977) *Eur. J. Biochem. 78*, 403–409.

500-MHz ^1H NMR Study of Poly(dG)·Poly(dC) in Solution Using One-Dimensional Nuclear Overhauser Effect†

Mukti H. Sarma, Goutam Gupta, and Ramaswamy H. Sarma*

Institute of Biomolecular Stereodynamics, State University of New York at Albany, Albany, New York 12222

Received December 26, 1985; Revised Manuscript Received February 11, 1986

ABSTRACT: Secondary structures of poly(dG)·poly(dC) and poly(dG)·poly(dm^5C) in solution are determined by nuclear Overhauser effect (NOE) measurements on GH8-deuterated and -nondeuterated DNAs with low presaturation pulse lengths (10–25 ms) and low-power and prolonged accumulations in the range of 50 000–72 000 scans. Under these conditions, the NOE difference spectra were free from diffusion. Primary NOEs between base protons GH8/CH6 and sugar protons H1′, H2′/H2″, and H3′ suggest that in poly(dG)·poly(dC) both guanine and cytosine nucleotides adopt a C3′-endo, low anti χ = 200–220° conformation. Computer modeling of the NOE data enable identification for the first time, in terms of the geometry of the nucleotide repeat, handedness, and helix geometry, of the structure of poly(dG)·poly(dC) to be the A form, and the derived structure for the polymer duplex is very close to the single crystal structure of the double-helical d-GGGGCCCC [McCall, M., Brown, T., & Kennard, O. (1985) *J. Mol. Biol. 183*, 385–396]. Similar nuclear Overhauser effect data on poly(dG)·poly(dm^5C) revealed that G and m^5C adopt a C2′-endo, anti χ = 240–260° conformation, which indicates that this DNA exhibits the B form in solution. In summary, the results presented in this paper demonstrate that methylation of cytosines in poly(dG)·poly(dC) causes A → B transition in the molecule.

Single-crystal and fiber diffraction studies have clearly demonstrated that, depending upon base sequence and environmental conditions, DNA can assume the right-handed A and B forms or the left-handed Z form (Arnott et al., 1975, 1983; Connor et al., 1982; Drew et al., 1980; Fratini et al., 1982; Kennard, 1985; McCall et al., 1985; Shakked et al., 1983; Viswamitra et al., 1982; Wang et al., 1979, 1982; Wing et al., 1980). NMR studies on DNA polymer duplexes in solution have revealed the presence of B and Z forms (Dhingra et al., 1983; Mitra et al., 1981a,b; Patel et al., 1982). However, the presence of the A form for a DNA polymer duplex in ordinary solution conditions of salt and water has not been unequivocally established—this is not surprising because high humidity is expected to favor the classical B form, and hence, in ordinary solution conditions of salt and water one expects the B form.

† This research is supported by the National Institutes of Health (GM29787) and the National Foundation for Cancer Research. We thank Y. P. Myer for providing access to the CD machine. The high-field NMR experiments were performed at the NMR Facility for Biomolecular Research located at the Francis Bitter National Magnet Laboratory, MIT. The NMR Facility is supported by Grant RR0095 from the Division of Research Resources of the NIH and by the National Science Foundation under Contract C-670.

0006-2960/86/0425-3659$01.50/0

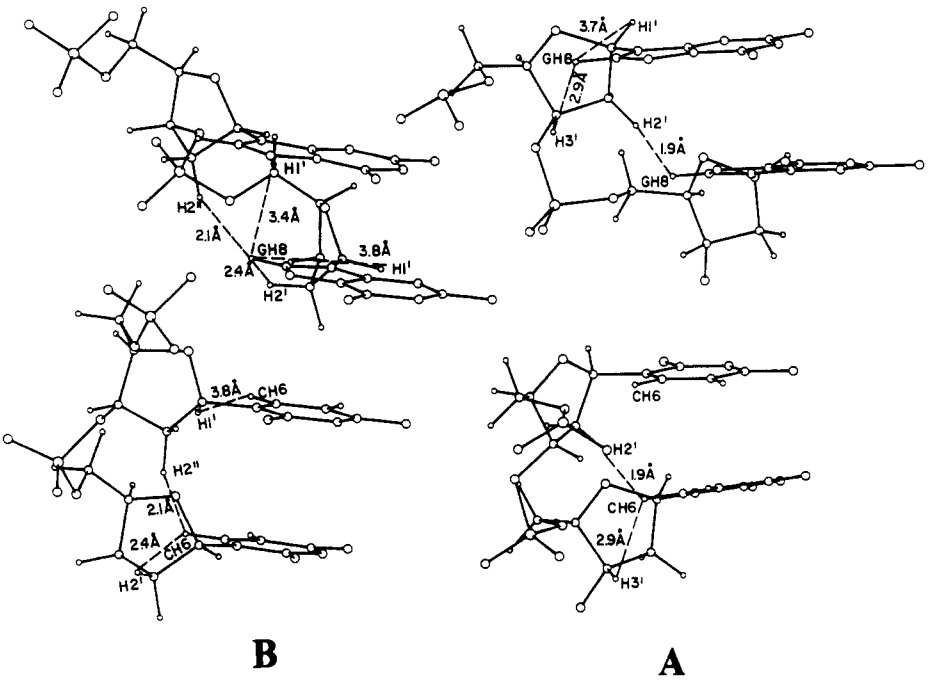

FIGURE 1: (A) Relevant interproton distances (less than 4 Å) for G (top) and C (bottom) nucleotides when the nucleotide geometry belongs to the C3′-endo, χ = 200–220° domain. Distances between the base protons GH8 and CH6 and sugar protons H1′, H2′/H2″, and H3′ are GH8/CH6---H1′ of the same nucleotide = 3.7 Å, GH8/CH6---H2′ of the neighboring nucleotide = 1.9Å, and GH8/CH6---H3′ of the same nucleotide = 2.9 Å. In this domain, torsion angle δ (C5′–C4′–C3′–O3′), which defines the ring pucker, can vary between 70 and 100° and χ (C4Pu–N9Pu–C1′–O1′) can vary between 200–220°. But for all combinations of δ and χ, the interproton distances follow the same pattern as shown in the figure. It must be emphasized that in the A-form distances between GH8/CH6 and H2′/H2″ of its own nucleotide unit or H2″ of the neighboring residue are beyond 4 Å. (B) Relevant interproton distances (less than 4 Å) for G (top) and C (bottom) nucleotides when the nucleotide geometry belongs to the C2′-endo, χ = 240–260° domain. Distances (below 4 Å) between the base protons GH8/CH6 and sugar protons H1′, H2′/H2″, and H3′ are GH8/CH6---H1′ of the same nucleotide = 3.8 Å, GH8/CH6---H1′ of the neighboring nucleotide = 3.4 Å, GH8/CH6---H2′ of the same nucleotide = 2.4 Å, and GH8/CH6---H2″ of the neighboring nucleotide 2.1 Å.

Recent demonstration that DNA oligonucleotides of sequences d-GGGGCCCC, d-GGCCGGCC, and d-CCGG (Kennard et al., 1985; McCall et al., 1985; Wang et al., 1982; Conner et al., 1982) in hydrated crystals exhibit the A form prompted us to search for the A form in aqueous solution for poly(dG)·poly(dC). NOE spectroscopy was used because this methodology clearly enables one to determine the conformation of the individual nucleotidyl unit, and this is considerably different for the A and B forms of DNA. In addition, it was of obvious interest to examine the effect of cytosine methylation at C5 on the conformation of poly(dG)·poly(dC) because methylation in other DNAs has been reported to cause conformational transitions (Behe & Felsenfeld, 1981; Fujii et al., 1982).

Materials and Methods

Poly(dG)·poly(dC) and poly(dG)·poly(dm^{5}C) were obtained from P-L Biochemicals. They were sonicated as described elsewhere (Sarma et al., 1984) except that the time of sonication was increased from 30 min to 3.5 h. The length of the polynucleotide as determined by alkaline agarose gel electrophoresis with standard markers was found to be 200 ± 50 base pairs. In vitro deuteration of GH8 of guanine in the polymers was performed as described elsewhere (Sarma et al., 1984). Solution conditions for the various NMR experiments are given in the legends of the appropriate figures.

Results and Discussion

Identification of Two Favored Nucleotide Conformations in DNA: Use of 1D NOE. The nucleotide unit with C3′-endo, χ = 200–220° conformation[1] represents the structural motif of A DNA, and the nucleotide unit with C2′-endo, χ = 240–260° conformation embodies the structural motif of B DNA (Berthod & Pullman, 1973; Day et al., 1973; Sasisekharen, 1973; Sundarlingam, 1975; Wilson, 1975). Therefore, identification of nucleotide geometry in terms of sugar pucker and glycosyl torsion helps us, in effect, to identify the polymorphous forms of DNA. Two nucleotide geometries—C3′-endo, χ = 200–220° and C2′-endo, χ = 240–260°—are distinguished from each other by a set of interproton distances between the base protons H8/H6 and the sugar protons H1′, H2′/H2″, H3′. 1D NOE spectroscopy provides an excellent method for examining the difference in the interproton distances in the two nucleotide geometries (Figure 1) and thereby making a clear identification of one of the two nucleotide geometries. For details of methodology, refer to Gupta et al. (1985, 1986) and Sarma et al. (1985).

Poly(dG)·Poly(dC) Adopts A Form in Solution. Figure 2 shows the low-field region of the 500-MHz ^{1}H NMR spectra of poly(dG)·poly(dC) at 30 and 60 °C. At 30 °C, CH6 and GH8 overlap, and at 60 °C they separate; after GH8 was exchanged with deuterium, the spectrum was recorded at 60 °C, which revealed that CH6 occurs at a lower field than GH8 (Figure 2, bottom panel). Other protons, viz., CH1′, GH1′, CH5, CH3′, GH3′, CH2′/H2″, and GH2′/H2″, were assigned from several NOE experiments conducted at 60 °C (Figure 3). Notice that at 30 °C H3′ protons are hidden under the HDO peak (Figure 2); however, they come clear of the HDO peak at 40 °C. All NOE experiments for structure determination were done at 30 or 40 °C. These were the lowest possible temperatures at which the desired experiments can be conducted on poly(dG)·poly(dC). In the temperature range of 30–60 °C, the spectra of poly(dG)·poly(dC) in water were monitored in the region of exchangeable protons (i.e., –NH

[1] Nomenclature follows IUB–IUPAC recommendations.

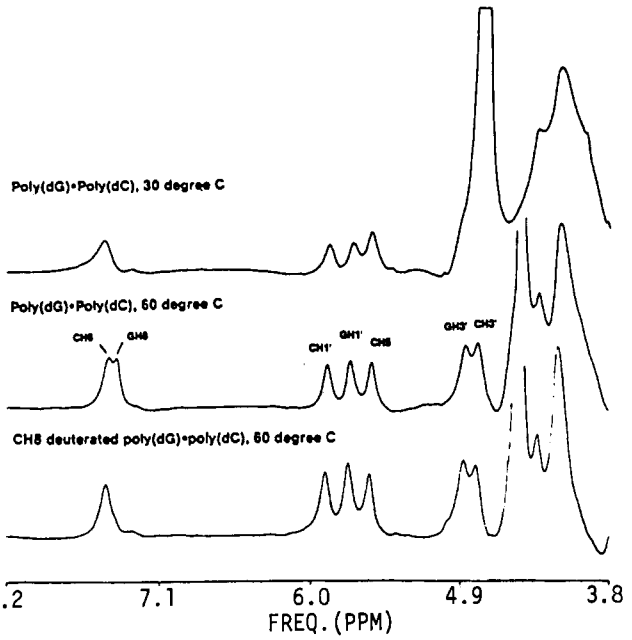

FIGURE 2: Low-field region of the 500-MHz ^1H NMR spectra of poly(dG)·poly(dC) at 30 (a) and 60 °C (b) and that of C(8)-deuterated poly(dG)·poly(dC) at 60 °C (c). The concentration of DNA was 15.00 mM in phosphates in 2.5 mM sodium phosphate buffer, pH 7.0, 100 mM NaCl, and 2.5 mM EDTA. The assignments indicated are discussed in the legend for Figure 3. In spectrum c, CH8 of G has been exchanged out by deuterium. In the spectrum at 60 °C, the GH8 and CH6 clearly separate, and the H3′ region emerges out of the HDO signal. At 30 °C, the only discernable change is that GH8 and CH6 merge together and move to a slightly lower field.

and $-NH_2$), which revealed that the DNA was entirely double helical in this temperature range.

As discussed elsewhere (Gupta et al., 1985, 1986; Sarma et al., 1985) in polymeric DNA, spin–diffusion (secondary and higher order NOE) tends to mask the primary NOE pattern. However, the primary NOE sites could be isolated from the spin–diffused ones by monitoring NOE as a function of presaturation pulse length. As one lowers the presaturation length, the sites of spin–diffusion begin to diminish in intensity. For poly(dG)·poly(dC) at 30 and 40 °C, we were able to record the NOE difference spectra at a presaturation pulse length of 10 ms, and the observed NOE pattern was essentially primary in nature.

As shown in Figure 2, GH8 and CH6 overlap at 30–40 °C; by simple presaturation of the combined GH8/CH6 signals and observation of the NOE at the sugar protons, the individual nucleotide geometries of G and C could not be identified. However, this apparent problem was circumvented by specifically deuterating GH8 and using the *GH8-deuterated* sample to identify the nucleotide geometry of C. Spectrum b of Figure 4 shows the difference NOE spectrum in which CH6 of GH8-deuterated poly(dG)·poly(dC) is presaturated for 10 ms: the primary sites of NOE are CH5, CH1′, and one of the two signals from CH2′/CH2″ (compare Figure 4b with Figures 3ab and 4a). Strong NOE at one of the two signals from CH2′/CH2″ suggests that C nucleotides in poly(dG)·poly(dC) adopt a C3′-endo, χ = 200–220° conformation and that CH2′ lies at a field higher than CH2″ in Figure 3a,b.

From Figure 1A it is clear that for a C3′-endo, χ = 200–220° conformation one expects an NOE at H3′ from CH6/GH8 (distance CH6/GH8---H3′ = 2.9 Å). However, at 30 °C both CH3′ and GH3′ signals of poly(dG)·poly(dC) are hiddent under HDO, and hence, from spectrum b of Figure 4, it is technically difficult to observe an NOE at the H3′

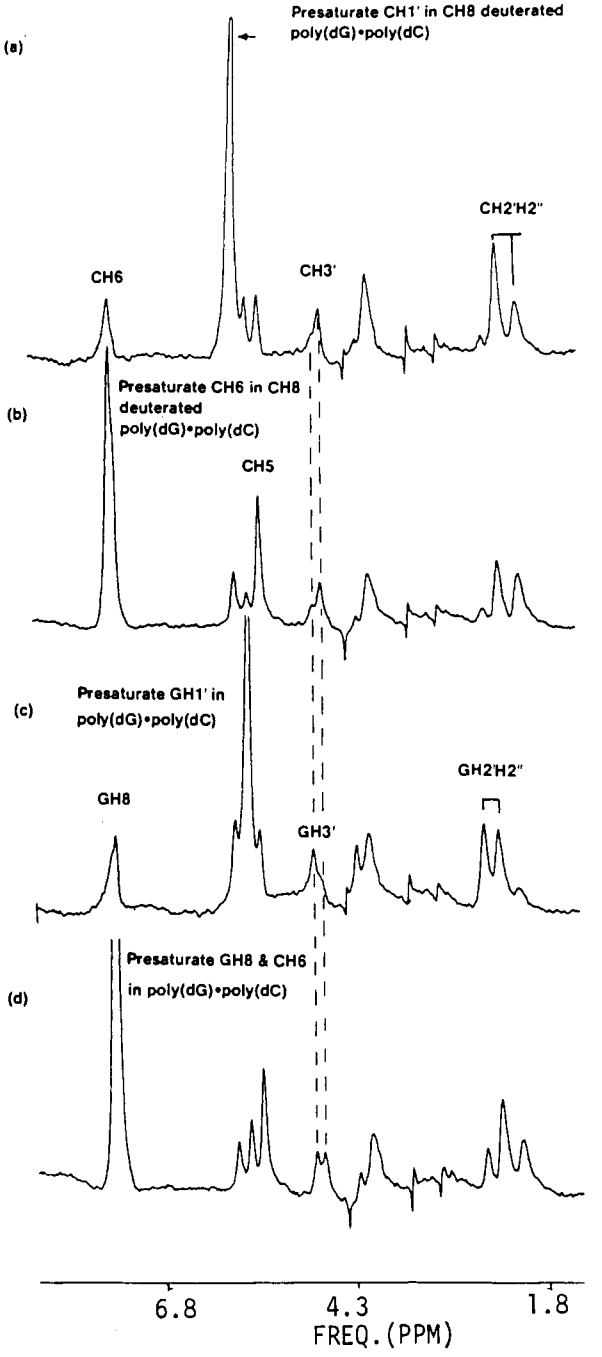

FIGURE 3: Assignments of protons in poly(dG)·poly(dC). The principle of our assignment by spin–diffusion is the following: in a two-stranded nonalternating system such as poly(dG)·poly(dC), if one presaturates a proton in one strand at long presaturation pulse lengths, all the protons of the *same* strand will receive magnetization transfer by diffusion along the strand so much so all protons of the same strand will show strong NOEs; there cannot be direct diffusion from one strand to another because the WC hydrogen-bonded protons are deuterated; so, diffusion to the second strand should come from intermolecular aggregation, and such diffusions are discernably small. The crux of the assignment is that at 60 °C GH8 and CH6 appear separately and both of them can be unambiguously assigned by selective deuteration (Figure 2). Once this is done, the rest of the protons in each strand can be correlated to CH6 or GH8 by diffusion along each strand. The four spectra in this figure clearly illustrate how this is accomplished. At first, CH6 is irradiated in the GH8-deuterated sample of poly(dG)·poly(dC), and CH5 and CH1′ are assigned. Then, CH1′ is irradiated to identify CH2′, H2″, CH3′, CH4′, H5′, and H5″. Similar experiments are performed on poly(dG)·poly(dC) to identify GH1′, GH2′, H2″, GH3′, GH4′, H5′, and H5″. Notice that two C2′-methylene protons—one belonging to G and other belonging to C—partially overlap in the spectrum.

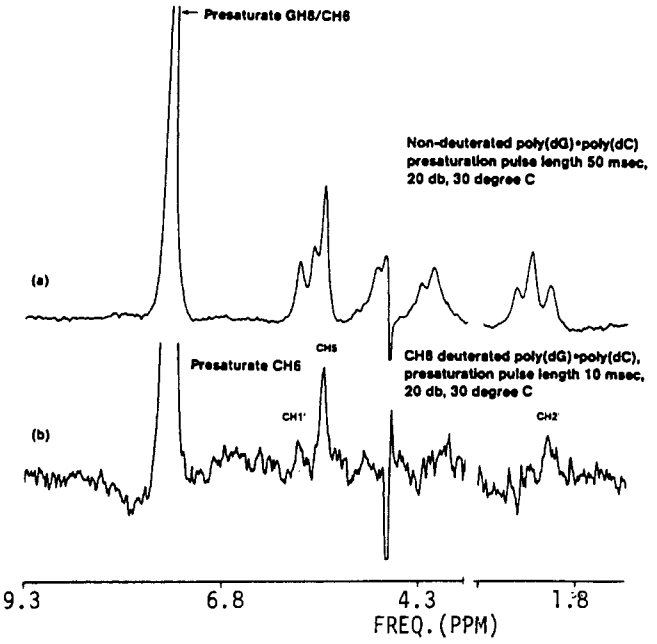

FIGURE 4: (Spectrum a) NOE difference spectrum of poly(dG)•poly(dC) at 30 °C in which both GH8 and CH6 were presaturated at 50 ms, 20 dB. The spectrum is very close to the corresponding one at 60 °C (i.e., spectrum d in Figure 3), indicating that assignment derived for 60 °C holds true also for 30 °C. (Spectrum b) NOE difference spectrum of *GH8-deuterated* poly(dG)•poly(dC) at 30 °C in which CH6 is presaturated; presaturation time and power were 10 ms and 20 dB, respectively. Number of scans was 46 000, which took 49 h. The spectrum obtained is free from spin–diffusion (compare with Figures 3a and 4a). It must be emphasized that at the employed conditions of 10-ms presaturation pulse length there is no diffusion from CH2′ to CH2″. The primary sites of NOEs from CH6 are CH1′, CH5, and CH2′, which are only consistent with the C3′-endo, χ = 200–220° conformation for nucleotide C (Figure 1A) but not with the C2′-endo, χ = 240–260° conformation of C (Figure 1B).

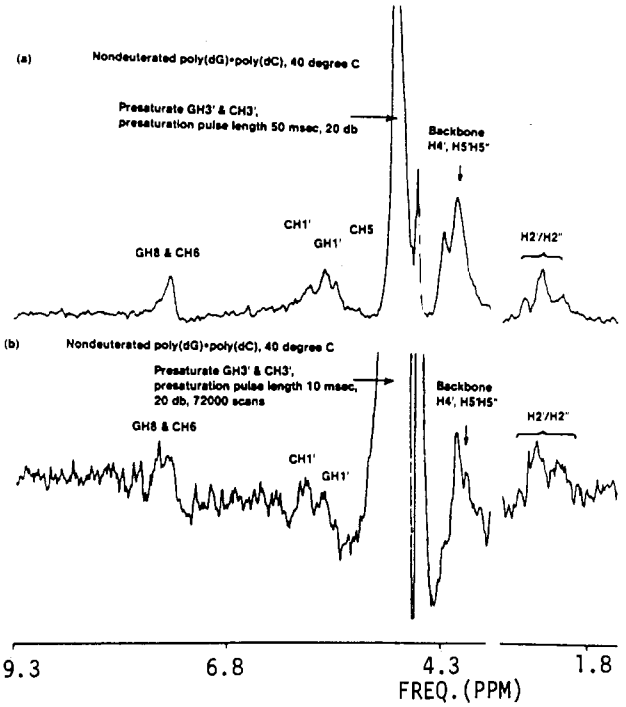

FIGURE 5: (Spectrum a) NOE difference spectrum of poly(dG)•poly(dC) at 40 °C in which GH3′ and CH3′ are presaturated at 50 ms, 20 dB. Note that the temperature has to be raised from 30 to 40 °C so that H3's could be irradiated without simultaneously presaturating HDO peak. However, GH3′ and CH3′ at 40 °C were too close in chemical shift to be individually presaturated, and hence, GH3′/CH3′ combined was presaturated. (Spectrum b) NOE difference spectrum of poly(dG)•poly(dC) at 40 °C in which GH3′/CH3′ combined is presaturated at 10 ms, 20 dB; number of scans was 72 000. The primary sites of NOE from GH3′/CH3′ are GH8/CH6, CH1′, GH1′, and other sugar protons. NOEs from GH3′ and CH3′ to the base protons GH8 and CH6 clearly suggest that both G and C nucleotide adopt C3′-endo, χ = 200–220° conformation, as in A DNA.

region. In order to verify whether GH3′ and CH3′ are indeed close to GH8 and CH6, difference NOE spectra of poly(dG)•poly(dC) were recorded at 40 °C when GH3′ and CH3′ come clear of the HDO signal. Spectra a and b Figure 5 are the NOE spectra of poly(dG)•poly(dC) in which GH3′/CH3′ combined has been presaturated for 50 and 10 ms, respectively, at 40 °C. As mentioned earlier, for 10 ms of presaturation time one essentially records the primary NOE pattern. The presence of NOE in Figure 5 from H3′ to base protons GH8/CH6 is explicable only if both G and C nucleotides adopt a C3′-endo, χ = 200–220° conformation as in A DNA.

The results in Figures 4 and 5 give direct evidence that both G and C nucleotides in poly(dG)•poly(dC) adopt a C3′-endo, χ = 200–220° conformation as in the A form of DNA. It may be noted that Arnott et. al. (1975) has demonstrated that A DNA is the only stable form exhibited by poly(dG)•poly(dC) in fibers. CD spectra of poly(dG)•poly(dC) were recorded under various conditions (data not shown).[2] The characteristic features of the spectra were as follows. The ratio of the positive band at 257 nm to the negative band at 238 nm (at 30 °C) is 5.0—a characteristic of the A form. The CD spectrum of poly(dG)•poly(dC) recorded after adding ethanol up to 70% by volume showed no change, suggesting that this DNA was already locked in the A conformation (Gray & Ratliff, 1975). A small hump at 290 nm, which is not present in the classical A form of calf thymus DNA, is always present within a temperature range of 20–70 °C for poly(dG)•poly(dC) and, hence, is likely to be a distinctive feature, i.e., effect of base composition and base sequence. Thus, from the results of Figures 4 and 5 along with the CD data it can be said that poly(dG)•poly(dC) in solution adopts the A form with both G and C nucleotides in the C3′-endo, χ = 200–220° conformation.

Poly(dG)•Poly(dm^{5}C) Adopts B Form in Solution. In the case of poly(dG)•poly(dm^{5}C), NMR measurements were conducted in the temperature range of 50–70 °C depending upon the protons presaturated. Because of resonance overlap and line broadening, the lowest temperature at which one could obtain a reasonable spectrum was 50 °C. In the employed temperature range of 50–70 °C, this DNA remained completely double helical as monitored by the Watson–Crick NH signals in water. The lowest presaturation pulse length which one could employ and obtain a reasonable NOE difference spectra in 50 h was 25 ms. Under these conditions, as it will become evident later, the spectra were free from diffusion.

Figure 6 shows the low-field region of the 500-MHz ^{1}H NMR spectrum of poly(dG)•poly(dm^{5}C) at 50 °C. Notice that GH8 and CH6 overlap and so do GH1′ and CH1′. At 50 °C, GH3′ and CH$_3$′ are hidden under the HDO peak, but at 70 °C, they come clear of the HDO signal (see the inset). Therefore, for poly(dG)•poly(dm^{5}C) we performed NOE experiments at two separate temperatures: at 50 °C when the GH8/CH6 signal was irradiated and NOEs were monitored at H1′ and H2′/H2″ and at 70 °C when GH3′/CH3′ combined was irradiated and NOEs were monitored in the base proton GH8/CH6 region. Spectra a and b in Figure 7 show the NOE pattern in poly(dG)•poly(dm^{5}C) when GH8/CH6

[2] CD spectra were removed during revision to save space upon requests from the editors; however, they can be obtained from the authors upon request.

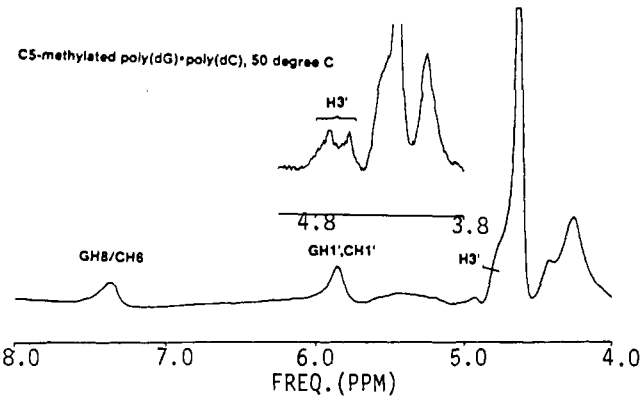

FIGURE 6: Low-field region of 500-MHz ^1H NMR spectrum of poly(dG)·poly(dm^{5}C) at 50 °C. Note that GH1′ and CH1′ as well as GH8 and CH6 resonances merge together. The inset indicates the H3′ region at 70 °C when HDO moves away, exposing the H3′ protons.

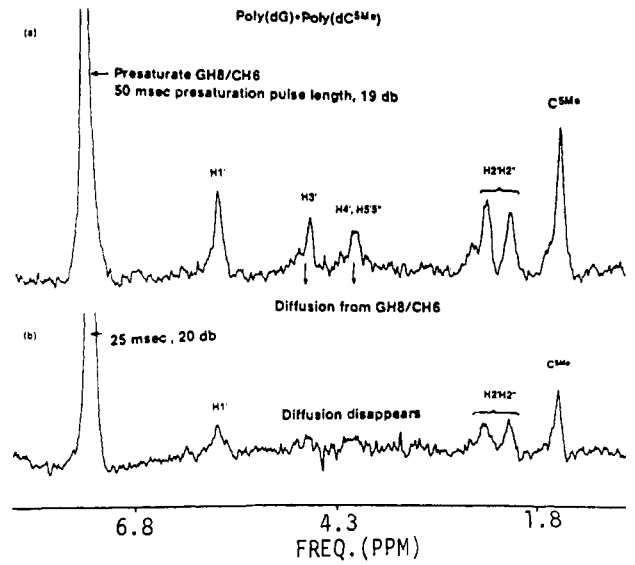

FIGURE 7: (Spectrum a) NOE difference spectrum of poly(dG)·poly(dm^{5}C) at 50 °C when GH8 and CH6 were presaturated at 50 ms, 19 dB; number of transients was 32 000. The assignments are obvious by inspection because most of the protons of G and C residues have the same chemical shifts (ppm) at 50 °C: GH8/CH6 = 7.34, GH1′/CH1′ = 5.75, GH3′/CH3′ = 4.68, GH2′H2″/CH2′H2″ = 2.62–2.15, and m^{5}C = 1.52. It should be noted that at 70 °C (inset of Figure 7) the H3′ protons of G and C residues resolve to separate positions at 4.74 and 4.60 ppm; this is not the case at 50 °C. (Spectrum b) NOE difference spectrum of poly(dG)·poly(dm^{5}C) at 50 °C when GH8 and CH6 were presaturated at 25 ms, 20 dB; number of scans was 56 680; it took 49 h to complete the data accumulation. Notice that the sites of spin–diffusion present in spectrum b have disappeared here. The primary sites of NOE from GH8/CH6 are H1′, H2′H2″, and m^{5}C as expected from the interproton distances for C2′-endo, χ = 240–260° (Figure 1B), as in B DNA. Note that there is no NOE to the H3′ region, thus ruling out the possibility of a C3′-endo, χ = 200–220° conformation as in A DNA (Figure 1A).

is irradiated for 50 and 25 ms, respectively. The NOE spectrum b for 25 ms of presaturation time is free of spin–diffusion; the primary sites of NOE from GH8/CH6 are H1′, H2′/H2″, and CH3.

The observed NOE pattern at the H2′/H2″ and m^{5}C region is the typical signature for the B form of DNA (Gupta et al., 1985, 1986; Sarma et al., 1985), a situation in which an equally strong NOE appears at H2′ and H2″ when the base proton GH8 or CH6 is presaturated (Figure 1B). Because GH2′/H2″ and CH2′/H2″ overlap, we have repeated the experiments in Figure 7 using *GH8-deuterated* poly(dG)·poly(dm^{5}C) in which CH6 was presaturated. In this case also, we observed

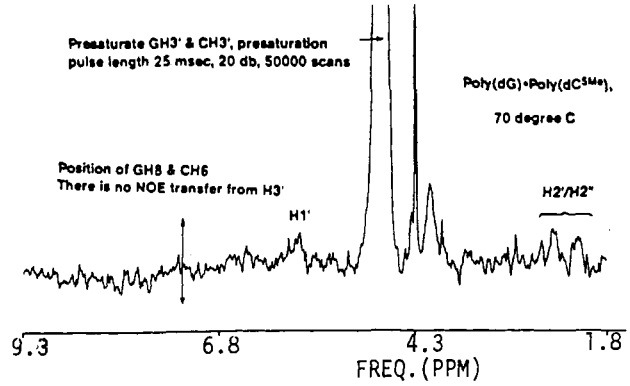

FIGURE 8: NOE difference spectrum of poly(dG)·poly(dm^{5}C) when the H3′ region has been irradiated at 25 ms, 20 dB, conditions under which there is very little spin–diffusion (see spectrum b of Figure 7); 50 000 transients were recorded (for 49 h) for this spectrum. Notice that there is no NOE from H3′ to the base protons GH8/CH6, thereby ruling out the possibility of C3′-endo, χ = 200–220° conformation for both G and C. This NOE difference spectrum of poly(dG)·poly(dm^{5}C) provides a contrast to that of poly(dG)·poly(dC) in Figure 5.

magnetization transfer from CH6 to CH1′, CH2′/H2″, and m^{5}C as in spectrum b of Figure 7. These observations clearly indicate that the nucleotide geometries of G and C residues in poly(dG)·poly(m^{5}C) belong to the B family, i.e., C2′-endo, χ = 240–260°. If the nucleotide geometry belonged to the A family, i.e., C3′-endo, χ = 200–220°, one indeed would have observed transfer of magnetization from GH8/CH6 to H3′ region. One does not see this in spectrum b of Figure 7, which is free from spin–diffusion. One can reconfirm this by performing a reverse NOE experiment in which GH3′/CH3′ were presaturated. Figure 8 shows the NOE difference spectrum of poly(dG)·poly(dm^{5}C) at 70 °C when GH3′ and CH3′ were presaturated. The data clearly show that no NOE is observed at GH8/CH6 from GH3′/CH3′. The NOE difference spectra in Figure 8 stand in sharp contrast to that in Figure 5 where one observes NOE transfer from H3′ to the base protons. The results in Figures 7 and 8 are consistent only with a nucleotide geometry of C2′-endo, χ = 240–260°, i.e., B helix, for poly(dG)·poly(dm^{5}C).

The CD spectrum of poly(dG)·poly(dm^{5}C) was recorded at 60 °C (data not shown);[2] the ratio of the positive band at 256 nm to the negative band at 236 nm is 1.4, which is characteristic of the B form. A small hump in the 280–310-nm region, which is not present in the classical B form of calf thymus DNA, is always present for poly(dG)·poly(dm^{5}C) within 20–70 °C and thus may be considered an effect of base composition and base sequence. Thus, by combining the NOE (Figures 7 and 8) and CD results, one can conclude that poly(dG)·poly(dm^{5}C) forms a B helix in solution with G and C nucleotides adopting a C2′-endo, χ = 240–260° conformation.

Comparison with Crystal Structure Data. NOE data presented in the previous sections suggest that poly(dG)·poly(dC) in solution adopts a right-handed A-DNA duplex with dG/dC in the C3′-endo, χ = 200–220° conformation while poly(dG)·poly(dm^{5}C) displays a right-handed B-DNA duplex in solution with dG/dm^{5}C in the C2′-endo, χ 240–260° conformation. Having obtained the nucleotide geometries, the final A-DNA/B-DNA model of poly(dG)·poly(dC)/poly(dG)·poly(dm^{5}C) was obtained subject to the following constraints: (i) the helical parameters, i.e., n, number of base pair per turn, and h, height per base pair, were fixed at n = 11, h = 2.56 Å) for A DNA and n = 10, h = 3.40 Å for B DNA; (ii) δ—the torsion angle describing the sugar pucker—was

Table I: Conformational Parameters (deg) for Two Models of Poly(dG)·Poly(dC) in A Form: Model Deduced from NOE Data and from Crystal Data of $d(GGGGCCCC)_2$

torsion angles[a]	present model from NOE data of d(GpG)/d(CpC)	model from crystal data of d(GpG)/d(CpC)[b]
ϵ (C4′–C3′–O3′–P)	193	204
ξ (C3′–O3′–P–O5′)	300	290
α (O3′–P–O5′–C5′)	288	294
β (P–O5′–C5′–C4′)	185	178
γ (O5′–C5′–C4′–C3′)	50	62
δ (C5′–C4′–C3′–O3′)	79	84
χ (O1′–C1′–N9G–C4G)	207	202
χ (O1′–C1′–N1C–C2C)	207	202

[a] IUB–IUPAC nomenclature has been used for the torsion angles. [b] Correspond to the average values for d(GpG) and d(CpC); there are very little differences in the conformational parameters for the dG and dC residues in the crystal structure (McCall et al., 1985).

Table II: Conformational Parameters (deg) for B-DNA Models of Poly(dG)·Poly(dm^5C)

torsion angles[a]	present model from NOE data of d(GpG)/ d(m^5Cpm^5C)	fiber model of d(GpG)/ d(m^5Cpm^5C)[a]
ϵ (C4′–C3′–O3″–P)	223	219
ξ (C3′–O3′–P–O5′)	212	203
α (O3′–P–O5′–C5′)	310	327
β (P–O5′–C5′–C4′)	149	138
γ (O5′–C5′–C4′–C3′)	42	138
δ (C5′–C4′–C3′–O3′)	139	33
χ (O1′–C1′–N9G–C84G)	253	250
χ (O1′–C1′–N1C–C2C)	253	250

[a] The conformational parameters for the fiber B-DNA model (Arnott et al., 1983; Sasisekharan et al., 1983) and B_{II} conformation of the dodecamer (Fratini et al., 1982) are very similar.

varied within the C3′-endo domain ($70° \leq \delta \leq 100°$) for A DNA and C2′-end domain ($120° \leq \delta \leq 160°$) for B DNA; (iii) χ—the glycosyl torsion—was varied within 200–220° for A DNA and 240–260° for B DNA; (iv) other torsion angles $\alpha, \beta, \gamma, \epsilon, \zeta$ were also allowed to vary simultaneously such that the resulting A-DNA/B-DNA models were free of steric compression; (v) it was always ensured that all the models retained the interproton distances as required by the NOE data. Table I lists the conformational parameters for one of the A-DNA models of poly(dG)·poly(dC) in solution which satisfy the criteria i–v; corresponding parameters for the A-DNA model deduced from the single-crystal data of $d(GGGGCCCC)_2$ (McCall et al., 1985) are also included for comparison. Notice the striking similarity between the solution model and that deduced from the crystal data. Figure 9 shows the (pdGpdG)·(pdCpdC) fragment in the A-DNA model viewed along and down the helix axis. Notice that the bases are tilted with respect to the helix axis and displaced away from the helix center such that they fall on the peripheri of the helix. Table II lists the conformational parameters for the B-DNA model of poly(dG)·poly(dm^5C) in solution; corresponding parameters for the B_{II} conformation of the dodecamer (Fratini et al., 1982), and the fiber B-DNA model (Arnott et al., 1983; Sasisekharan et al., 1983), are also given for comparison. Our solution B-DNA model is very similar to the B_{II} conformation of the dodecamer and the fiber B-DNA model. Figure 10 shows the (pdGpdG)·(pdm^5Cpdm^5C) fragment in the final B-DNA model projected along and down the helix axis. Notice that the bases are almost perpendicular to the helix axis and are situated very close to the helix center. Compare Figures 9 and 10 to visualize the changes in the stacking brought about by methylation of C in poly(dG)·poly(dC)

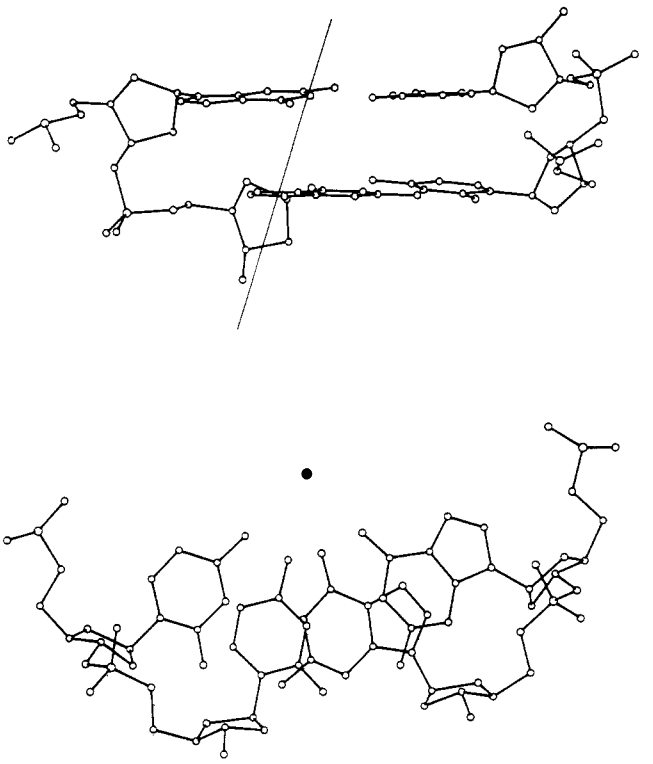

FIGURE 9: (pdGpdG)·(pdCpdC) fragment in the final A-DNA model ($n = 11$, $h = 2.56$ Å) of poly(dG)·poly(dC). In this model, both G and C nucleotides adopt C3′-endo, $\chi = 200$–220° conformation. (Top) View along the helix axis, which shows that bases do have a considerable tilt (20°); (bottom) view down the helix axis, which shows that bases are displaced away from the helix center (by about 4 Å).

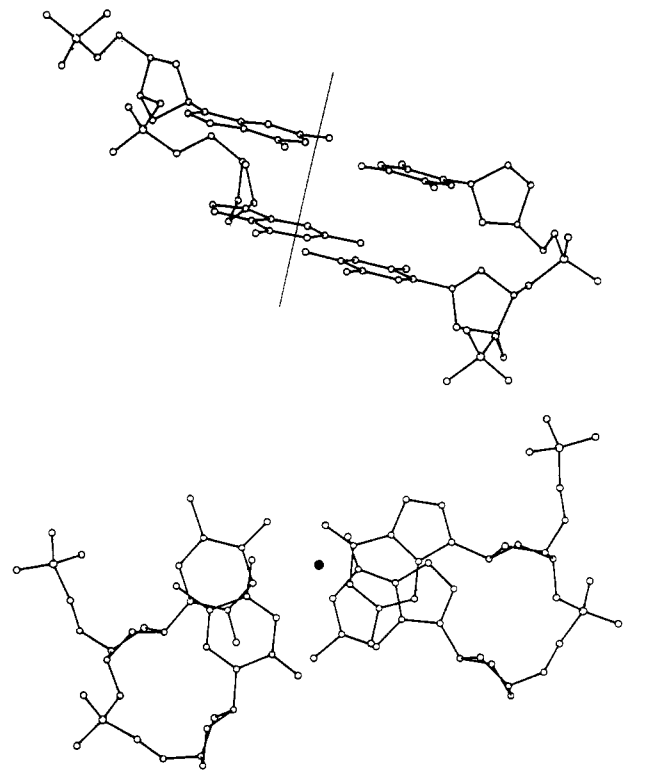

FIGURE 10: (pdGpdG)·(pdm^5Cpdm^5C) fragment of the final B-DNA model ($n = 10$, $h = 3.40$ Å) of poly(dG)·poly(dm^5C) viewed along and down the helix axis. Notice that upon methylation bases are moved away from the peripheri towards the inner core of the helix concomitant with A → B transition.

concomitant with the A → B transition: upon methylation in poly(dG)·poly(dC), both G and C move from the peripheri

to the inner core of the helix. Even though in poly(dG)·poly(dC) only one strand is chemically modified, both strands show structural change. To the best of our knowledge, this is the first report that shows m^5C can cause A → B transition in DNA.

Registry No. m^5C, 554-01-8; poly(dG)·poly(dC), 25512-84-9; poly(dG)·poly(dm^5C), 90150-74-6.

REFERENCES

Arnott, S., Chandrasekharan, R., & Selsing, E. (1975) in *Structure and Conformation of Nucleic Acids and Protein-Nucleic Acid Interactions* (Sundarlingam, M., & Rao, S. T., Eds.) pp 577–596, University Park Press, Baltimore, MD.

Arnott, S., Chandrasekaran, R., Puigjaner, L. C., & Walker, S. K. (1983) in *Nucleic Acids: Vectors of Life* (Pullman, B., & Jortner, J., Eds.) pp 17–31, Reidel, Dordrecht, The Netherlands.

Behe, M., & Felsenfeld, G. (1981) *Proc. Natl. Acad. Sci. U.S.A. 78*, 7010–7014.

Berthod, H., & Pullman, B. (1973) *FEBS Lett. 33*, 147–152.

Connor, B. N., Takano, T., Tanaka, S., Itakura, K., & Dickerson, R. E. (1982) *Nature (London) 295*, 294–299.

Day, R. O., Seeman, N. C., Rosenberg, J. M., & Rich, A. (1973) *Proc. Natl. Acad. Sci. U.S.A. 70*, 849–853.

Dhingra, M. M., Sarma, M. H., Gupta, G., & Sarma, R. H. (1983) *J. Biomol. Struct. Dyn. 1*, 417–428.

Drew, H., Takano, T., Tanaka, S., Itakura, K., & Dickerson, R. E. (1980) *Nature (London) 286*, 567–573.

Fratini, A. V., Kopka, M. L., Drew, H. R., & Dickerson, R. E. (1982) *J. Biol. Chem. 257*, 14686–14707.

Fujii, S., Wang, A. H.-J., van der Marel, G., van Boom, J. H., & Rich, A. (1982) *Nucleic Acids Res. 10*, 7879–7892.

Gray, D., & Ratliff, R. (1975) *Biopolymers 14*, 487–498.

Gupta, G., Sarma, M. H., & Sarma, R. H. (1985) *J. Mol. Biol. 186*, 463–469.

Gupta, G., Sarma, M. H., & Sarma, R. H. (1986) *Int. J. Quantum Chem., Quantum Biol. Symp. No. 12*, 183–199.

Kennard, O. (1985) *J. Biomol. Struct. Dyn. 3*, 205–226.

McCall, M., Brown, T., & Kennard, O. (1985) *J. Mol. Biol. 183*, 385–396.

Mitra, C. K., Sarma, M. H., & Sarma, R. H. (1981a) *Biochemistry 20*, 2036–2041.

Mitra, C. K., Sarma, M. H., & Sarma, R. H. (1981b) *J. Am. Chem. Soc. 103*, 6727–6737.

Patel, D. J., Kozlowski, S., Nordheim, A., & Rich, A. (1982) *Proc. Natl. Acad. Sci. U.S.A. 79*, 1413–1417.

Sarma, M. H., Gupta, M. H., & Sarma, R. H. (1985) *J. Biomol. Struct. Dyn. 2*, 1057–1084.

Sasisekharan, V. (1973) *Jerusalem Symp. Quantum Chem. Biochem. 5*, 247–251.

Sasisekharan, V., Bansal, B., & Gupta, G. (1983) in *Nucleic Acids: Vectors of Life* (Pullman, B., & Jortner, S., Eds.) pp 101–111, Reidel, Dordrecht, The Netherlands.

Shakked, Z., Rabinovich, D., Cruse, W. B. T., Kennard, O., Salisbury, S. A., & Viswanitra, M. A. (1982) *J. Mol. Biol. 166*, 183–201.

Sundarlingam, M. (1975) in *Structure and Conformation of Nucleic Acids and Protein-Nucleic Acid Interaction* (Sundarlingam, M., & Rao, S. T., Eds.) pp 487–524, University Park Press, Baltimore, MD.

Viswamitra, M. A., Shakked, Z., Jones, P. G., Sheldrick, G. M., Salisbury, S. A., & Kennard, O. (1982) *Biopolymers 21*, 513–532.

Wang, A. H.-J., Quigley, G. A., Kolpak, F. J., Crawford, J. L., van Boom, J. H., van der Marel, G., & Rich, A. (1979) *Nature (London) 282*, 680–686.

Wang, A. H.-J., Fujii, S., van Boom, J. H., & Rich, A. (1982) *Proc. Natl. Acad. Sci. U.S.A. 79*, 3968–3972.

Wilson, H. R. (1975) in *Structure and Conformation of Nucleic Acids and Protein-Nucleic Acid Interactions* (Sundarlingam, M., & Rao, S. T., Eds.) pp 525–536, University Park Press, Baltimore, MD.

Wing, R., Drew, H., Takano, T., Broka, C., Tanaka, S., Itakura, K., & Dickerson, R. E. (1980) *Nature (London) 287*, 755–758.